UNIVERSITÄT AUGSBURG
Universitätsbibliothek

OPEN ACCESS
OPUS AUGSBURG

Experimental evidence for importance of Hund's exchange interaction for incoherence of charge carriers in iron-based superconductors

J. Fink, E. D. L. Rienks, S. Thirupathaiah, J. Nayak, A. van Roekeghem, S. Biermann, T. Wolf, P. Adelmann, Hirale S. Jeevan, Philipp Gegenwart, S. Wurmehl, C. Felser, B. Büchner

Angaben zur Veröffentlichung / Publication details:

Fink, J., E. D. L. Rienks, S. Thirupathaiah, J. Nayak, A. van Roekeghem, S. Biermann, T. Wolf, et al. 2017. "Experimental evidence for importance of Hund's exchange interaction for incoherence of charge carriers in iron-based superconductors." *Physical Review B* 95 (14): 144513. https://doi.org/10.1103/physrevb.95.144513.

Nutzungsbedingungen / Terms of use:

licgercopyright

Dieses Dokument wird unter folgenden Bedingungen zur Verfügung gestellt: / This document is made available under these conditions:
Deutsches Urheberrecht
Weitere Informationen finden Sie unter: / For more information see:
https://www.uni-augsburg.de/de/organisation/bibliothek/publizieren-zitieren-archivieren/publiz/

Experimental evidence for importance of Hund's exchange interaction for incoherence of charge carriers in iron-based superconductors

J. Fink,[1,2,3,*] E. D. L. Rienks,[1,3] S. Thirupathaiah,[4] J. Nayak,[2] A. van Roekeghem,[5] S. Biermann,[6,7] T. Wolf,[8] P. Adelmann,[8] H. S. Jeevan,[9,†] P. Gegenwart,[9] S. Wurmehl,[1,3] C. Felser,[2] and B. Büchner[1,3]

[1]*Leibniz Institute for Solid State and Materials Research Dresden, Helmholtzstr. 20, D-01069 Dresden, Germany*
[2]*Max Planck Institute for Chemical Physics of Solids, D-01187 Dresden, Germany*
[3]*Institut für Festkörperphysik, Technische Universität Dresden, D-01062 Dresden, Germany*
[4]*Solid State and Structural Chemistry Unit, Indian Institute of Science, Bangalore, Karnataka 560012, India*
[5]*CEA, LITEN, 17 Rue des Matyrs, 38054 Grenoble, France*
[6]*Centre de Physique Théorique, Ecole Polytechnique, 91128 Palaiseau Cedex, France*
[7]*LPS, Université Paris Sud, Bâtiment 510, 91405 Orsay, France*
[8]*Karlsruhe Institute of Technology, Institut für Festkörperphysik, 76021 Karlsruhe, Germany*
[9]*Institut für Physik, Universität Augsburg, Universitätstr. 1, D-86135 Augsburg, Germany*

(Received 27 October 2016; published 25 April 2017)

Angle-resolved photoemission spectroscopy is used to study the scattering rates of charge carriers from the hole pockets near Γ in the iron-based high-T_c hole-doped superconductors $K_xBa_{1-x}Fe_2As_2$, $x = 0.4$, and $K_xEu_{1-x}Fe_2As_2$, $x = 0.55$, and the electron-doped compound $Ba(Fe_{1-x}Co_x)_2As_2$, $x = 0.075$. The scattering rate for any given band is found to depend linearly on the energy, indicating a non-Fermi-liquid regime. The scattering rates in the hole-doped compound are considerably higher than those in the electron-doped compounds. In the hole-doped systems the scattering rate of the charge carriers of the inner hole pocket is about three times higher than the binding energy, indicating that the spectral weight is heavily incoherent. The strength of the scattering rates and the difference between electron- and hole-doped compounds signals the importance of Hund's exchange coupling for correlation effects in these iron-based high-T_c superconductors. The experimental results are in qualitative agreement with theoretical calculations in the framework of combined density functional dynamical mean-field theory.

DOI: 10.1103/PhysRevB.95.144513

I. INTRODUCTION

Originally iron-based superconductors (FeSC) [1] were believed to exhibit only moderate electronic Coulomb correlations because x-ray absorption data derived an on-site Coulomb interaction U of less than 2 eV [2,3]. More recent theoretical work [4–9], however, emphasizes that, in contrast to the cuprates, where the correlation effects are dominated by U, in the FeSCs—because of their intrinsically multiorbital character—there is another factor to consider: the Hund exchange interaction J_H.

Angle-resolved photoemission spectroscopy (ARPES) is a suitable method to obtain information on the strength of correlation effects since it delivers the energy (E) and momentum ($\mathbf{k}$)-dependent self-energy function $\Sigma(E,\mathbf{k})$, from which one can derive the mass enhancement and the scattering rate of the charge carriers due to many-body effects [10,11].

There are numerous experimental studies on the mass enhancement in FeSC's using various methods which apparently support the strong influence of correlation effects, in particular, related to Hund's exchange interaction. A recent compilation of such data was published in Ref. [12]. The effective masses show a remarkably large variance; e.g., the effective mass of KFe_2As_2 varies between 2 and 19. There are two reasons for these uncertainties: (i) the derived effective masses are related to the theoretical values of the bare mass, usually taken from a DFT band structure calculation; and (ii) there are several ARPES studies [13–17] indicating that the mass renormalization is energy dependent (enhanced at low energies), which, for methods covering different energy ranges, leads to different values for the effective mass.

Recently, ARPES studies on the scattering rate or the lifetime broadening $\Gamma(E)$ of electron-doped FeSC's, equal to twice the imaginary part of the self-energy $\Im\Sigma(E)$, have been presented by several groups [15,18–22]. To our knowledge, no studies of the energy dependence of $\Gamma(E)$ in hole-doped FeSCs exist in the literature. Besides the orbital dependencies of the scattering rate, the temperature-dependent crossover from coherent quasiparticles to incoherent charge carriers is believed to provide support for a new metallic phase, which was dubbed Hund's metal [7]. Reference [9] theoretically predicted that the regime should be associated with a characteristic energy dependence of the lifetimes of elementary excitations, in particular, not following the parabolic behavior, which is a hallmark of the Fermi liquid. Within a model context, such behavior was investigated within high-precision renormalization-group techniques in Ref. [23] and interpreted as an intermediate "spin-orbitally separated" regime, where screened orbital degrees of freedom are coupled to slowly fluctuating spins that are not yet Kondo screened. At very low temperatures, a crossover to a Fermi-liquid regime is expected. On the other hand, in any normal metal there is a crossover from a Fermi-liquid to an incoherent behavior at higher temperatures when the lifetime broadening Γ exceeds the binding energy of the charge carriers. Therefore, experimental

*j.fink@ifw-dresden.de
†Present address: Department of Physics, PESITM, Sagar Road, 577204 Shimoga, India.

 ©2017 American Physical Society

work is needed to investigate the nature of the bad metallic phase, to identify the intermediate regime, to check the theoretical predictions, and to analyze the energy dependence of the scattering rates.

In this contribution we use ARPES to study the scattering rates in hole-doped "122" ferropnictides $K_xBa_{1-x}Fe_2As_2$ and $K_xEu_{1-x}Fe_2As_2$ and compare the results with those derived from our previous ARPES experiments [15,21,24,25] on electron-doped compounds. The essential result of the present study is that the linear-in-energy non-Fermi-liquid scattering rates in hole-doped compounds are considerably higher than in electron-doped compounds. We ascribe the high scattering rates in the hole-doped compounds, different from the cuprates, to the proximity to a compound with a $3d^5$ configuration in which, similarly to Mn compounds, Hund's exchange interaction J_H is important for the correlation effects. The ARPES results are in qualitative agreement with our calculations in the framework of DFT combined with dynamical mean-field theory (DMFT).

II. EXPERIMENTAL PROCEDURE

Single crystals were grown using the self-flux technique and characterized by transport and thermal property measurements [26–28]. ARPES measurements were conducted at the 1^3-ARPES endstation attached to the beamline UE112 PGM 2 at BESSY, with energy and angle resolutions between 4 and 15 meV and 0.2°, respectively. Variable photon energies $h\nu = 20$–130 eV were used to reach different k_z values in the Brillouin zone. The use of polarized photons allows the selection of spectral weights with a specific orbital character by matrix element effects [29].

III. THEORY

We have performed combined density functional/dynamical mean-field theory (DFT + DMFT) calculations [30,31] using the DFT + DMFT implementation in Ref. [5]. We have chosen the local density approximation to the exchange-correlation functional, and Hubbard and Hund's interactions obtained from the constrained random phase approximation [32] in the implementation of Ref. [33]. The constrained random phase approximation calculations [34] yield $F^0 = 2.6$ eV, $F^2 = 6.2$ eV, and $F^4 = 4.7$ eV, corresponding to a Hund's rule coupling of $J_H = 0.8$ eV. Calculations were performed at an inverse temperature of 100 eV^{-1}, corresponding to 116 K. The DMFT equations were solved using a continuous-time quantum Monte Carlo solver [35] as implemented in the TRIQS package [36], followed by an analytical continuation procedure using the maximum entropy algorithm [37].

IV. RESULTS

In the present contribution we focus on the scattering rates of charge carriers from hole pockets and, in particular, from the inner hole pocket. The reason for this is that in previous studies of electron-doped and P-substituted compounds, $\Gamma(E)$ was found to be strongest for the inner hole pocket [15]. Moreover, the superconducting gap is largest for the inner

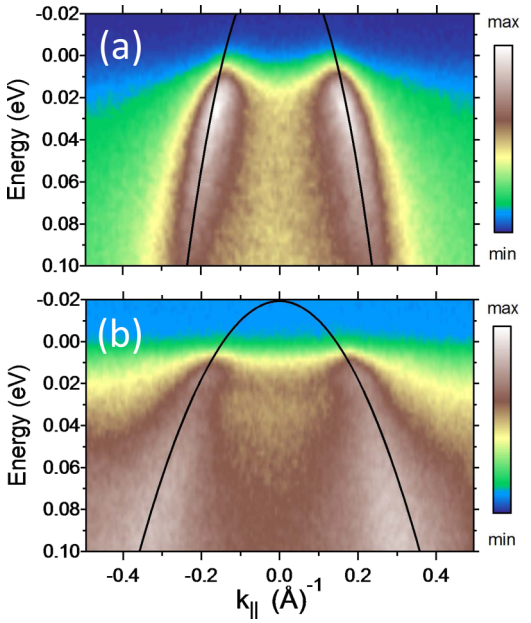

FIG. 1. Energy distribution maps of the hole pockets of $K_xBa_{1-x}Fe_2As_2$, $x = 0.4$, near the center of the Brillouin zone, measured along the Γ-M direction. Black lines indicate the derived band dispersion. (a) Spectral weight of the inner hole pocket measured at a temperature of $T = 40$ K using vertically polarized photons with an energy of 75 eV. (b) Spectral weight of the middle hole pocket measured at $T = 1.5$ K using horizontally polarized photons with an energy of 47 eV.

hole pocket [38,39]. In Fig. 1 we show representative data on the spectral weight of the inner [Fig. 1(a)] and the middle [Fig. 1(b)] hole pockets near the center of the Brillouin zone of optimally doped $K_xBa_{1-x}Fe_2As_2$, $x = 0.4$, with a superconducting transition temperature $T_c = 30$ K. Along this direction the inner hole pocket has a predominantly Fe $3d_{yz}$ character, while the middle hole pocket has a predominantly Fe $3d_{xz}$ character [15]. The inner hole pocket is measured in the normal state to avoid the influence of the superconducting gap. For the middle hole pocket we present data in the superconducting state to show the Bogoliubov-like back dispersion near the Fermi level. The intensity of the outer hole pocket with a predominantly Fe $3d_{xy}$ character is very weak in this compound because bands with this orbital character exhibit the highest elastic scattering rates [40].

Similar energy distribution maps were obtained on overdoped $K_xEu_{1-x}Fe_2As_2$, $x = 0.55$ ($T_c = 29$ K) (not shown). Data on the slightly overdoped $Ba(Fe_{1-x}Co_x)_2As_2$, $x = 0.075$ ($T_c = 22$ K), for the inner two hole pockets near Γ were already presented in previous publications [21,24,25]. Also, in this compound only the inner two hole pockets are visible at the Γ point, and not the outer one.

We have analyzed the ARPES data by a new method using a two-dimensional fit of the measured spectral function $A(E,k)$ [11]. In this way we derived the dispersion, approximated by a polynomial and $\Im\Sigma(E)$. We have avoided using one of the standard evaluation methods. The first method consists in fitting cuts at a constant energy (momentum distribution curves) by Lorentzians. To obtain the scattering rates $\Gamma(E)$ the widths in

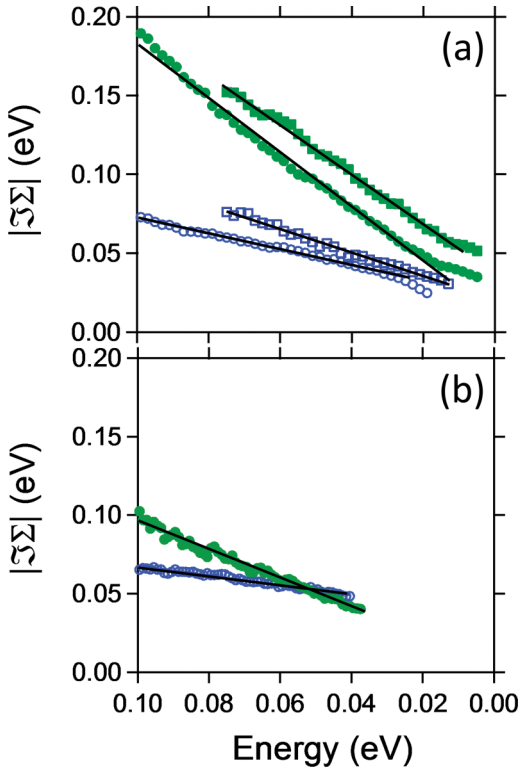

FIG. 2. $\Im\Sigma$ as a function of the binding energy for the inner hole pocket (filled green symbols, upper curves) and for the middle hole pocket (open blue symbols, lower curves). (a) Data for hole-doped $K_xBa_{1-x}Fe_2As_2$, $x = 0.4$ (circles), and $K_xEu_{1-x}Fe_2As_2$, $x = 0.55$ (squares). (b) Data for electron-doped $Ba(Fe_{1-x}Co_x)_2As_2$, $x = 0.075$. The inner hole pocket data for $K_xBa_{1-x}Fe_2As_2$ and the $K_xEu_{1-x}Fe_2As_2$ data were measured at $T = 40$ K. The middle hole pocket data for $K_xBa_{1-x}Fe_2As_2$ and $Ba(Fe_{1-x}Co_x)_2As_2$ were measured at 1.5 K. Black lines are derived from a linear fit.

momentum space are multiplied by the *renormalized* velocity. As shown in the Supplemental Material [11] the method is only correct for dispersions with small curvatures and for a small energy dependence of $\Im\Sigma$. In the second method the momentum distribution curve widths are multiplied by the *bare* particle velocity to derive $\Im\Sigma$ for the *coherent* part of the spectral weight. This is correct for systems in which the coherent spectral weight is well separated from the incoherent spectral weight and is mainly located in satellites [10,41,42]. As shown below, in the ferropnictides as well as in other correlated systems such as the cuprates, even near the Fermi level, a large part of the spectral weight is incoherent and therefore it is only possible to derive $\Gamma(E)$ or $\Im\Sigma(E)$ from the sum of coherent and incoherent charge carriers. Using our new evaluation method we also avoid having to account for the bare particle velocity, which is, in principle, unknown and which is usually taken from DFT calculations.

In this way we obtain $\Im\Sigma(E,k)$ for the two inner hole pockets of $K_xBa_{1-x}Fe_2As_2$, $x = 0.4$, $K_xEu_{1-x}Fe_2As_2$, $x = 0.55$, and $Ba(Fe_{1-x}Co_x)_2As_2$, $x = 0.075$, depicted in Fig. 2. In certain energy ranges $\Im\Sigma$ can be described by a linear-in-energy relationship $\Im\Sigma = \alpha + \beta E$. At low energy the data are limited by the finite energy resolution ($\approx$4 meV), by thermal excitations for data taken at finite temperatures in the normal state [see Fig. 2(a)] and for measurements in the superconducting state by three times the superconducting gap Δ (for $K_xBa_{1-x}Fe_2As_2$, $x = 0.4$, $\Delta \approx 6$ meV) [43]. Correspondingly, for bands which are separated from the Fermi level by an energy E_s and for which the lowest electron hole excitations are determined by a gap with an energy E_g, the lowest scattering processes appear at $E_s + E_g$ (for the slightly overdoped $Ba(Fe_{1-x}Co_x)_2As_2$, $x = 0.075$, $E_g \approx 25$ meV). On the high-energy side, the data are limited by the crossing of other bands. The constant term α is due to elastic scattering of the charge carriers, e.g., by the dopants or by contamination of the surface. The coefficient β of the linear term, absent in a normal Fermi liquid, is, however, a strong indicator of the strength of correlation effects. For $K_xBa_{1-x}Fe_2As_2$ we derive β values of 1.7 ± 0.2 and 0.5 ± 0.1 for the inner and the middle hole pocket, respectively. Similar values for β have been obtained for $K_xEu_{1-x}Fe_2As_2$, $x = 0.55$ ($\beta = 1.6 \pm 0.2$ and 0.7 ± 0.1 for the inner and the middle hole pocket, respectively). Comparing the data on overdoped $K_xEu_{1-x}Fe_2As_2$ with those on the optimally doped $K_xBa_{1-x}Fe_2As_2$, within error bars we do not observe a dopant dependence of the β values. This result is similar to that on electron-doped compounds [15]. The derived α values for $K_xEu_{1-x}Fe_2As_2$ are slightly larger than those for $K_xBa_{1-x}Fe_2As_2$, probably due to the higher impurity concentration. For the electron-doped compound $Ba(Fe_{1-x}Co_x)_2As_2$ we obtain β values of 0.8 ± 0.1 and 0.3 ± 0.05 for the inner and the middle hole pocket, respectively. These β values are similar to those derived for the electron-doped compounds $NaFe_{1-x}Co_xAs$ and $NaFe_{1-x}Rh_xAs$ [15]. The statistical error bar for the data points in Fig. 2 are of the order of the size of the symbols. The systematic errors of the β values are discussed in the Supplementary Material [11].

V. DISCUSSION

The linear-in-energy increase in $\Im\Sigma(E)$ signals no evidence of a coupling to bosonic excitations. If, e.g., phonons determined $\Im\Sigma$, a steplike increase should be observed at phonon energies close to 40 meV [41]. Moreover, similarly to the electron-doped and the P-substituted systems [15], no kinks are observed in the dispersion of the hole-doped compound $K_xBa_{1-x}Fe_2As_2$.

In a normal Fermi liquid the scattering rate should be proportional to E^2 [42]. Various ways of reaching non-Fermi-liquid regimes have been discussed in the literature. In Ref. [14], it was argued that the correlation-induced enhanced phase space for electronic excitations could lead to a linear-in-energy increase in the scattering rates. When the percentage of the coherent quasiparticles approaches 0, a marginal Fermi liquid is reached [11,44] and $\Im\Sigma$ becomes linear in energy. In this case dispersions observed in ARPES experiments should not be mistaken for a quasiparticle dispersion. The same is true of the Hund's metal regime discussed below.

Generally the validity of the quasiparticle description was defined by the equation $\frac{\Gamma}{E} = 2\beta \lessapprox 1$ [45]. The observed β values between 0.5 and 1.7 show that $\frac{\Gamma}{E}$ is between 1.0 and 3.4, which is not smaller than 1. Thus the charge carriers in the hole pockets are close to incoherent or are completely incoherent, as in the hole-doped compounds. Therefore it makes no sense to

separate the spectral weight into coherent states and incoherent states. It also makes no sense to compare our data with normal-state transport properties, since these are related to less correlated charge carriers stemming from other sections of the Fermi surface. Nevertheless, the large superconducting gap in the inner hole pocket [38,46] signals that the electrons in that pocket contribute to the superconducting pairing. Finally, we emphasize that the reduced slope of $\Im\Sigma$ at low energies in the upper curve in Fig. 2(a) does not indicate a Fermi-liquid behavior at low energies. Rather it is caused by the finite energy resolution, by the elastic scattering term $\alpha \approx 12$ meV, and by the finite $\Im\Sigma$ at zero energy but at finite temperature, which, in a marginal Fermi-liquid model, amounts to ≈7 meV at 40 K [11].

It is interesting to compare the present data with results derived on the cuprates. ARPES experiments on $Bi_2Sr_2CaCu_2O_8$ along the nodal direction derived a β value of 0.75, which also signals the incoherent character of the charge carriers in these compounds [47].

The difference between the scattering rate of the inner hole pocket and that of the middle hole pocket has been predicted by theoretical calculations [48,49] and compared with experimental data for electron-doped and P-substituted compounds [15]. This difference is caused by the fact that the scattering rates between sections having the same orbital character are higher than those between sections having different orbital characters.

To obtain deeper insights into the nature of the non-Fermi-liquid regime in the present case and to derive an at least semiquantitative comparison of the experimental results with theory we have performed calculations in the framework of DFT + DMFT. The results are consistent with the expectation of a highly doping-dependent incoherent state [9] based on the "spin-orbital separation" scenario [23] induced by Hund's coupling [50]: while in a half-filled system J_H increases the Mott gap, the inverse is true at all other commensurate fillings [51,52], making the scattering rates strongly doping dependent as predicted in [9].

Results for the calculated $\Im\Sigma(E)$ are presented in Fig. 3. For the hole-doped compound, at higher energies, an almost linear-in-energy non-Fermi-liquid behavior with $\beta \approx 0.9$ is realized. One should note that DFT + DMFT averages the scattering rate for a given orbital character over the hole Brillouin zone, while in the present ARPES experiment only one particular direction was analyzed, along which the orbital character of the inner and the middle hole pocket is dominated by yz and xz states, respectively. Thus the DFT + DMFT calculation should be compared with the average value of the inner and the middle hole pocket from ARPES. The calculations for the electron-doped system yield scattering rates which are strongly

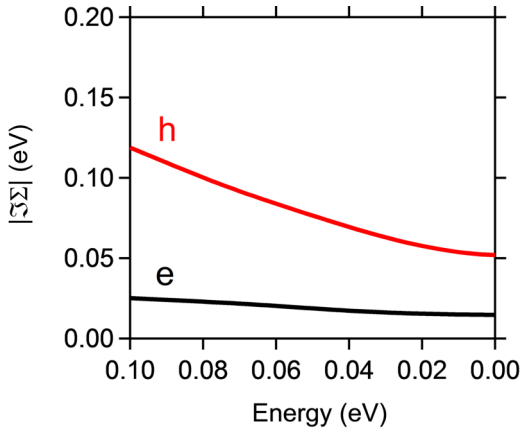

FIG. 3. DFT + DMFT calculations of $\Im\Sigma(E)$ as a function of the binding energy for electronic states having an xz/yz orbital character in $BaFe_2As_2$ with 0.2 hole/Fe (upper curve) and 0.075 electron/Fe (lower curve).

reduced. At high energies the calculations can be described by $\beta \approx 0.14$, much smaller than the measured values. This could indicate that the theoretical calculations still underestimate the correlation effects in these compounds.

VI. SUMMARY

Our study of the scattering rate of the charge carriers from the two inner hole pockets in iron-based superconductors reveals a non-Fermi-liquid region, consistent with previous observations in electron-doped compounds, now also in hole-doped compounds. The essential result of the present contribution is that most of the spectral weight in hole-doped systems is incoherent and that correlation effects strongly increase when going from electron- to hole-doped systems. These results emphasize the importance of Hund's exchange interaction for correlation effects in hole-doped FeSCs with a $3d$ count close to 5. The comparison with DFT + DMFT calculations yields almost-quantitative agreement for the hole-doped compound.

ACKNOWLEDGMENTS

This work was supported by the German Research Foundation, the DFG, through the priority program SPP 1458 and by the European Research Council (Consolidator Grant No. 617196) and IDRIS/GENCI Orsay (Project No. t2016091393). We thank Michele Casula for useful discussions. S.T. acknowledges support by the Department of Science and Technology through the INSPIRE-Faculty program (Grant No. IFA14 PH-86).

[1] D. C. Johnston, The puzzle of high temperature superconductivity in layered iron pnictides and chalcogenides, Adv. Phys. **59**, 803 (2010).

[2] T. Kroll, S. Bonhommeau, T. Kachel, H. A. Dürr, J. Werner, G. Behr, A. Koitzsch, R. Hübel, S. Leger, R. Schönfelder, A. K. Ariffin, R. Manzke, F. M. F. de Groot, J. Fink, H. Eschrig, B. Büchner, and M. Knupfer, Electronic structure of $LaFeAsO_{1-x}F_x$ from x-ray absorption spectroscopy, Phys. Rev. B **78**, 220502 (2008).

[3] W. L. Yang, A. P. Sorini, C.-C. Chen, B. Moritz, W.-S. Lee, F. Vernay, P. Olalde-Velasco, J. D. Denlinger, B. Delley, J.-H. Chu, J. G. Analytis, I. R. Fisher, Z. A. Ren, J. Yang, W. Lu,

Z. X. Zhao, J. van den Brink, Z. Hussain, Z.-X. Shen, and T. P. Devereaux, Evidence for weak electronic correlations in iron pnictides, Phys. Rev. B **80**, 014508 (2009).

[4] M. Aichhorn, S. Biermann, T. Miyake, A. Georges, and M. Imada, Theoretical evidence for strong correlations and incoherent metallic state in FeSe, Phys. Rev. B **82**, 064504 (2010).

[5] M. Aichhorn, L. Pourovskii, V. Vildosola, M. Ferrero, O. Parcollet, T. Miyake, A. Georges, and S. Biermann, Dynamical mean-field theory within an augmented plane-wave framework: Assessing electronic correlations in the iron pnictide LaFeAsO, Phys. Rev. B **80**, 085101 (2009).

[6] L. de'Medici, Hund's coupling and its key role in tuning multiorbital correlations, Phys. Rev. B **83**, 205112 (2011).

[7] K. Haule and G. Kotliar, Coherence-incoherence crossover in the normal state of iron oxypnictides and importance of Hund's rule coupling, New J. Phys. **11**, 025021 (2009).

[8] E. Razzoli, C. E. Matt, M. Kobayashi, X.-P. Wang, V. N. Strocov, A. van Roekeghem, S. Biermann, N. C. Plumb, M. Radovic, T. Schmitt, C. Capan, Z. Fisk, P. Richard, H. Ding, P. Aebi, J. Mesot, and M. Shi, Tuning electronic correlations in transition metal pnictides: Chemistry beyond the valence count, Phys. Rev. B **91**, 214502 (2015).

[9] P. Werner, M. Casula, T. Miyake, F. Aryasetiawan, A. J. Millis, and S. Biermann, Satellites and large doping and temperature dependence of electronic properties in hole-doped $BaFe_2As_2$, Nat. Phys. **8**, 331 (2012).

[10] A. Damascelli, Z. Hussain, and Z.-X. Shen, Angle-resolved photoemission studies of the cuprate superconductors, Rev. Mod. Phys. **75**, 473 (2003).

[11] See Supplemental Material at http://link.aps.org/supplemental/10.1103/PhysRevB.95.144513 for details on the analysis of the scattering rates.

[12] A. van Roekeghem, P. Richard, H. Ding, and S. Biermann, Spectral properties of transition metal pnictides and chalcogenides: Angle-resolved photoemission spectroscopy and dynamical mean-field theory, C.R. Phys. **17**, 140 (2016).

[13] H. Ding, K. Nakayama, P. Richard, S. Souma, T. Sato, T. Takahashi, M. Neupane, Y.-M. Xu, Z.-H. Pan, A. V. Fedorov, Z. Wang, X. Dai, Z. Fang, G. F. Chen, J. L. Luo, and N. L. Wang, Electronic structure of optimally doped pnictide $Ba_{0.6}K_{0.4}Fe_2As_2$: A comprehensive angle-resolved photoemission spectroscopy investigation, J. Phys. Condens. Matter **23**, 135701 (2011).

[14] J. Fink, Influence of Lifshitz transitions and correlation effects on the scattering rates of the charge carriers in iron-based superconductors, Europhys. Lett. **113**, 27002 (2016).

[15] J. Fink, A. Charnukha, E. D. L. Rienks, Z. H. Liu, S. Thirupathaiah, I. Avigo, F. Roth, H. S. Jeevan, P. Gegenwart, M. Roslova, I. Morozov, S. Wurmehl, U. Bovensiepen, S. Borisenko, M. Vojta, and B. Büchner, Non-Fermi-liquid scattering rates and anomalous band dispersion in ferropnictides, Phys. Rev. B **92**, 201106 (2015).

[16] Y. Lubashevsky, E. Lahoud, K. Chashka, D. Podolsky, and A. Kanigel, Shallow pockets and very strong coupling superconductivity in $FeSe_xTe_{1-x}$, Nat. Phys. **8**, 309 (2012).

[17] P. Starowicz, H. Schwab, J. Goraus, P. Zajdel, F. Forster, J. R. Rak, M. A. Green, I. Vobornik, and F. Reinert, A flat band at the chemical potential of a $Fe_{1.03}Te_{0.94}S_{0.06}$ superconductor observed by angle-resolved photoemission spectroscopy, J. Phys. Condens. Matter **25**, 195701 (2013).

[18] V. Brouet, D. LeBoeuf, P.-H. Lin, J. Mansart, A. Taleb-Ibrahimi, P. Le Fèvre, F. Bertran, A. Forget, and D. Colson, ARPES view of orbitally resolved quasiparticle lifetimes in iron pnictides, Phys. Rev. B **93**, 085137 (2016).

[19] H. Miao, Z. P. Yin, S. F. Wu, J. M. Li, J. Ma, B.-Q. Lv, X. P. Wang, T. Qian, P. Richard, L.-Y. Xing, X.-C. Wang, C. Q. Jin, K. Haule, G. Kotliar, and H. Ding, Orbital-differentiated coherence-incoherence crossover identified by photoemission spectroscopy in LiFeAs, Phys. Rev. B **94**, 201109(R) (2016).

[20] Y. J. Pu, Z. C. Huang, H. C. Xu, D. F. Xu, Q. Song, C. H. P. Wen, R. Peng, and D. L. Feng, Temperature-induced band selective localization and coherent-incoherent crossover in single-layer FeSe/Nb : $BaTiO_3/KTaO_3$, Phys. Rev. B **94**, 115146 (2016).

[21] E. D. L. Rienks, T. Wolf, K. Koepernik, I. Avigo, P. Hlawenka, C. Lupulescu, T. Arion, F. Roth, W. Eberhardt, U. Bovensiepen, and J. Fink, Electronic structure and quantum criticality in $Ba(Fe_{1-x-y}Co_xMn_y)_2As_2$, an ARPES study, Europhys. Lett. **103**, 47004 (2013).

[22] M. Yi, D. H. Lu, R. Yu, S. C. Riggs, J.-H. Chu, B. Lv, Z. K. Liu, M. Lu, Y.-T. Cui, M. Hashimoto, S.-K. Mo, Z. Hussain, C. W. Chu, I. R. Fisher, Q. Si, and Z.-X. Shen, Observation of Temperature-Induced Crossover to an Orbital-Selective Mott Phase in $A_xFe_{2-y}Se_2$ (A = K, Rb) Superconductors, Phys. Rev. Lett. **110**, 067003 (2013).

[23] K. M. Stadler, Z. P. Yin, J. von Delft, G. Kotliar, and A. Weichselbaum, Dynamical Mean-Field Theory Plus Numerical Renormalization-Group Study of Spin-Orbital Separation in a Three-Band Hund Metal, Phys. Rev. Lett. **115**, 136401 (2015).

[24] S. Thirupathaiah, S. de Jong, R. Ovsyannikov, H. A. Dürr, A. Varykhalov, R. Follath, Y. Huang, R. Huisman, M. S. Golden, Yu-Zhong Zhang, H. O. Jeschke, R. Valenti, A. Erb, A. Gloskovskii, and J. Fink, Orbital character variation of the Fermi surface and doping dependent changes of the dimensionality in $BaFe_{2-x}Co_xAs_2$ from angle-resolved photoemission spectroscopy, Phys. Rev. B **81**, 104512 (2010).

[25] S. Thirupathaiah, E. D. L. Rienks, H. S. Jeevan, R. Ovsyannikov, E. Slooten, J. Kaas, E. van Heumen, S. de Jong, H. A. Dürr, K. Siemensmeyer, R. Follath, P. Gegenwart, M. S. Golden, and J. Fink, Dissimilarities between the electronic structure of chemically doped and chemically pressurized iron pnictides from an angle-resolved photoemission spectroscopy study, Phys. Rev. B **84**, 014531 (2011).

[26] A. E. Böhmer, F. Hardy, L. Wang, T. Wolf, P. Schweiss, and C. Meingast, Superconductivity-induced re-entrance of the orthorhombic distortion in $Ba_{1-x}K_xFe_2As_2$, Nat. Commun. **6**, 7911 (2015).

[27] H. S. Jeevan, D. Kasinathan, H. Rosner, and P. Gegenwart, Interplay of antiferromagnetism, ferromagnetism, and superconductivity in $EuFe_2(As_{1-x}P_x)_2$ single crystals, Phys. Rev. B **83**, 054511 (2011).

[28] J. Maiwald, H. S. Jeevan, and P. Gegenwart, Signatures of quantum criticality in hole-doped and chemically pressurized $EuFe_2As_2$ single crystals, Phys. Rev. B **85**, 024511 (2012).

[29] J. Fink, S. Thirupathaiah, R. Ovsyannikov, H. A. Dürr, R. Follath, Y. Huang, S. de Jong, M. S. Golden, Y.-Z. Zhang, H. O. Jeschke, R. Valentí, C. Felser, S. Dastjani Farahani, M. Rotter, and D. Johrendt, Electronic structure studies of $BaFe_2As_2$ by

angle-resolved photoemission spectroscopy, Phys. Rev. B **79**, 155118 (2009).

[30] V. I. Anisimov, A. I. Poteryaev, M. A. Korotin, A. O. Anokhin, and G. Kotliar, First-principles calculations of the electronic structure and spectra of strongly correlated systems: Dynamical mean-field theory, J. Phys. Condens. Matter **9**, 7359 (1997).

[31] A. I. Lichtenstein and M. I. Katsnelson, *Ab initio* calculations of quasiparticle band structure in correlated systems: LDA^{++} approach, Phys. Rev. B **57**, 6884 (1998).

[32] F. Aryasetiawan, M. Imada, A. Georges, G. Kotliar, S. Biermann, and A. I. Lichtenstein, Frequency-dependent local interactions and low-energy effective models from electronic structure calculations, Phys. Rev. B **70**, 195104 (2004).

[33] L. Vaugier, H. Jiang, and S. Biermann, Hubbard U and Hund exchange J in transition metal oxides: Screening versus localization trends from constrained random phase approximation, Phys. Rev. B **86**, 165105 (2012).

[34] A. van Roekeghem, L. Vaugier, H. Jiang, and S. Biermann, Hubbard interactions in iron-based pnictides and chalcogenides: Slater parametrization, screening channels, and frequency dependence, Phys. Rev. B **94**, 125147 (2016).

[35] E. Gull, A. J. Millis, A. I. Lichtenstein, A. N. Rubtsov, M. Troyer, and P. Werner, Continuous-time Monte Carlo methods for quantum impurity models, Rev. Mod. Phys. **83**, 349 (2011).

[36] O. Parcollet, M. Ferrero, T. Ayral, H. Hafermann, I. Krivenko, L. Messio, and P. Seth, TRIQS: A toolbox for research on interacting quantum systems, Comput. Phys. Commun. **196**, 398 (2015).

[37] M. Jarrell and J. E. Gubernatis, Bayesian inference and the analytic continuation of imaginary-time quantum Monte Carlo data, Phys. Rep. **269**, 133 (1996).

[38] S.y V. Borisenko, V. B. Zabolotnyy, A. A. Kordyuk, D. V. Evtushinsky, T. K. Kim, I. V. Morozov, R. Follath, and B. Büchner, One-sign order parameter in iron based superconductor, Symmetry **4**, 251 (2012).

[39] K. Umezawa, Y. Li, H. Miao, K. Nakayama, Z.-H. Liu, P. Richard, T. Sato, J. B. He, D.-M. Wang, G. F. Chen, H. Ding, T. Takahashi, and S.-C. Wang, Unconventional Anisotropic s-wave Superconducting Gaps of the LiFeAs Iron-Pnictide Superconductor, Phys. Rev. Lett. **108**, 037002 (2012).

[40] A. Herbig, R. Heid, and J. Schmalian, Charge doping versus impurity scattering in chemically substituted iron-pnictides, Phys. Rev. B **94**, 094512 (2016).

[41] S. Engelsberg and J. R. Schrieffer, Coupled electron-phonon system, Phys. Rev. **131**, 993 (1963).

[42] G. D. Mahan, *Many-Particle Physics* (Kluwer Academic, Dordrecht, 2000).

[43] M. R. Norman and H. Ding, Collective modes and the superconducting-state spectral function of $Bi_2Sr_2CaCu_2O_8$, Phys. Rev. B **57**, R11089(R) (1998).

[44] C. M. Varma, Z. Nussinov, and W. van Saarloos, Singular or non-Fermi liquids, Phys. Rep. **361**, 267 (2002).

[45] G. Grimvall, *The Electron-Phonon Interaction in Metals* (North-Holland, Amsterdam, 1981).

[46] H. Ding, P. Richard, K. Nakayama, K. Sugawara, T. Arakane, Y. Sekiba, A. Takayama, S. Souma, T. Sato, T. Takahashi, Z. Wang, X. Dai, Z. Fang, G. F. Chen, J. L. Luo, and N. L. Wang, Observation of Fermi-surface-dependent nodeless superconducting gaps in $Ba_{0.6}K_{0.4}Fe_2As_2$, Europhys. Lett. **83**, 47001 (2008).

[47] T. Valla, A. V. Fedorov, P. D. Johnson, B. O. Wells, S. L. Hulbert, Q. Li, G. D. Gu, and N. Koshizuka, Evidence for quantum critical behavior in the optimally doped cuprate $Bi_2Sr_2CaCu_2O_{8+\delta}$, Science **285**, 2110 (1999).

[48] S. Graser, T. A. Maier, P. J. Hirschfeld, and D. J. Scalapino, Near-degeneracy of several pairing channels in multiorbital models for the Fe pnictides, New J. Phys. **11**, 025016 (2009).

[49] A. F. Kemper, M. M. Korshunov, T. P. Devereaux, J. N. Fry, H.-P. Cheng, and P. J. Hirschfeld, Anisotropic quasiparticle lifetimes in Fe-based superconductors, Phys. Rev. B **83**, 184516 (2011).

[50] L. de'Medici, J. Mravlje, and A. Georges, Janus-Faced Influence of Hund's Rule Coupling in Strongly Correlated Materials, Phys. Rev. Lett. **107**, 256401 (2011).

[51] L. de' Medici, *Weak and Strong Correlations in Fe Superconductors* (Springer International, Cham, Switzerland, 2015), pp. 409–441.

[52] D. van der Marel and G. A. Sawatzky, Electron-electron interaction and localization in d and f transition metals, Phys. Rev. B **37**, 10674 (1988).